

Electronic Sputtering of Nanodimensional Hydrogenated Amorphous Carbon and Copper Oxide Thin Films

S. Ghosh

Indian Institute of Technology Delhi, New Delhi-110 016

ABSTRACT

Electronic sputtering of carbon from hydrogenated amorphous carbon (*a-C:H/Si*) film and oxygen from copper oxide (*CuO/Si*) film at different electronic energy loss (S_e) value is reported. The sputtering is monitored by online elastic recoil detection analysis (ERDA) technique and the yield (sputtered atoms/incident ion) is determined. Two important results emerging out from this study are: (i) much higher yield of C and O from *a-C:H* and *CuO* films as compared to conventional kinetic sputtering and (ii) sputtering yield increases with increase in S_e in both the cases. These observations are understood on the basis of thermal spike model of ion-solid interaction.

Keywords: Swift heavy ion, electronic sputtering, elastic recoil detection analysis, thermal spike

1. INTRODUCTION

Impingement of energetic particles on a solid may result in the ejection of atoms or ionic species from the surface known as sputtering. Depending upon the energy of the incident ion and its charge state, sputtering process can be classified into three categories, namely (i) kinetic sputtering or collisional sputtering, (ii) electronic sputtering and (iii) potential sputtering. Kinetic sputtering is a consequence of the collision cascade produced by the incoming projectile and higher generation of recoil atoms within the target. Moving atoms in the cascade may eventually reach the surface, and provided that the kinetic energy is large enough to overcome the attractive potential of the solid, they may escape from the solid and get sputtered. This process is dominant when incident ion energy range is from keV to a few MeV, where nuclear energy loss S_n is the prime energy loss factor. However, the probability of such collision events drops down when the incident energy is higher such as tens to hundreds of MeV (as in the present case) and hence, the sputtering yield (sputtered atoms/incident ion) is expected to be low.

However, in this energy regime, sputtering yield sometimes (after certain energy threshold) becomes too high (1000 atoms/ion or more) and cannot be calculated on the basis of well-established sputtering formalism¹ based on the concept of collision. In this energy regime, the sputtering process is governed by electronic energy loss S_e , and hence, it is designated as electronic sputtering². The energy threshold of electronic sputtering strongly depends on the ion and solid combination. Moreover, if the projectile ion is multiply charged and is moving slowly, a particular form of electronic sputtering can take place which has been termed as potential

sputtering³. In this case, the potential energy stored in multiply charged ions (i.e., the energy necessary to produce an ion of this charge state from its neutral atom) is liberated when the ions recombine during impact on a solid surface (formation of hollow atoms). Potential sputtering has only been observed for certain target species and requires a minimum potential energy³. Up till now kinetic sputtering has been established as an essential process for many technological applications, such as (i) thin film deposition, (ii) sputter etching, (iii) ion milling, (iv) mass spectroscopy analysis of materials, etc. However, electronic and potential sputtering are still under fundamental study and need more focused research to bring their utility in real life.

The present work is based on electronic sputtering addressing the important issue of high sputtering yield. Different authors have reported electronic sputtering yield in different materials⁴⁻⁶ indicating very high yield ($\sim 10^5$ atoms/ion) in some cases. In case of *a-C:H* film, large sputtering yield of C and H have been reported^{3,5} and explained on the basis of thermal spike concept⁷. In case of copper nitride films also, the same model was applied to explain the high sputtering yield⁶. According to this model, a thermal spike develops in the electronic subsystem just after the passage of the ion. This eventually gets transferred to the lattice via electron-phonon coupling and a transient (\sim picosecond to subnanosecond time scale) temperature spike develops in the lattice subsystem. The mathematical formalism of the model is based on two coupled thermodynamic equations⁷, which show the dependence of lattice temperature on spatial and temporal distribution of energy. It is reported that the energy deposition is prominent due to primary ionization and excitation within

a zone of radial dimension of ~ 10 nm, and beyond this, energy deposition by δ electrons dominates. In this model, the initial energy density is taken from a spatial distribution function and Gaussian distribution of time⁸. In electronic subsystem, electronic heat diffusivity and effective electron-atom relaxation time (τ) play major role to transient ($\sim 10^{-15}$ s) temperature spike in the subsystem. The energy transfer to the lattice depends on the electron-phonon coupling factor (g), which is inversely proportional to τ . Finally, the spike temperature in the lattice is decided by its specific heat and thermal conductivity.

Depending on the energy transferred to the atomic subsystem and the reached temperature, specific phase changes can be induced like transition from solid-to-liquid phase or liquid-to-vapour phase. Sputtering may occur in any of these phase transition stages, either from molten phase or vapour phase⁹. However, the question of large sputtering yield still remains unanswered, though, there are many realistic figures reported by different authors based on thermal spike models⁹⁻¹¹. The effect may be purely mediated by electronic energy loss or there may be a small influence of nuclear energy loss also⁸ depending upon ion energy and the material under study. It was shown that the microstructure of solids plays a crucial role in electronic sputtering process^{5,12}. For thin solid films having nanogranular structure, the thermal energy may get confined within the smaller grains, resulting in larger sputtering yield.

In this paper, the authors have reported (i) electronic sputtering of carbon from hydrogenated amorphous carbon (a-C:H) films under irradiation of 80 MeV Ni^{8+} , 150 MeV Ag^{13+} and 200 MeV Au^{15+} ions and (ii) electronic sputtering of O from copper oxide for the same ions and energy is presented. Sputtering process is monitored online using elastic recoil detection analysis (ERDA) technique, which has been established as a unique tool to study the electronic sputtering of thin films^{3,14}. The results are discussed in the light of thermal spike mechanism.

2. EXPERIMENTAL

Three a-C:H/Si (300 nm) films of the same set were irradiated by 80 MeV Ni^{8+} , 150 MeV Ag^{13+} and 200 MeV Au^{15+} ions in a vacuum of 8×10^{-7} Torr, achieved by a cryopump-based vacuum system. Similarly, three CuO/float glass (210 nm) films of the same set were irradiated by the same ions. The deposition process of the films was same as reported earlier¹⁵. The electronic S_e and nuclear S_n energy loss values for each of these incident ions were calculated from computer simulation code SRIM¹⁶ and are given in Table 1. A large area ΔE - E telescope detector¹⁴ was employed to detect the recoil species coming from the films. Two-dimensional spectrum of ΔE versus E_{tot} (total energy, $\Delta E + E_{rest}$) was generated, which provided the discrimination of different elements present in the film as recoil energy bands as shown in Fig. 1.

The areal concentration of any element (N in atoms/cm²) of elements present in any film was deduced (within an error of 10 per cent) from the integral counts R of the recoil energy spectra, with the help of the following equation:

$$N = \frac{RSin\alpha}{N_p \left(\frac{d\sigma}{d\Omega} \right) \Omega} \quad (1)$$

where α is the target tilt angle, Ω is the solid angle subtended by the detector and $\frac{d\sigma}{d\Omega}$ is the Rutherford' recoil cross section. This is then plotted wrt to the incident ion fluence. The electronic sputtering yield or Y (atoms/ion) of any element present in the film was determined by using the following formula

$$Y(\text{atoms/ion}) = \frac{\Delta N(\text{atoms/cm}^2)}{\Delta f(\text{ions/cm}^2)} \quad (2)$$

Where, ΔN is the change in areal concentration (atoms/cm²) at two points (in the initial part of the plot) and Δf

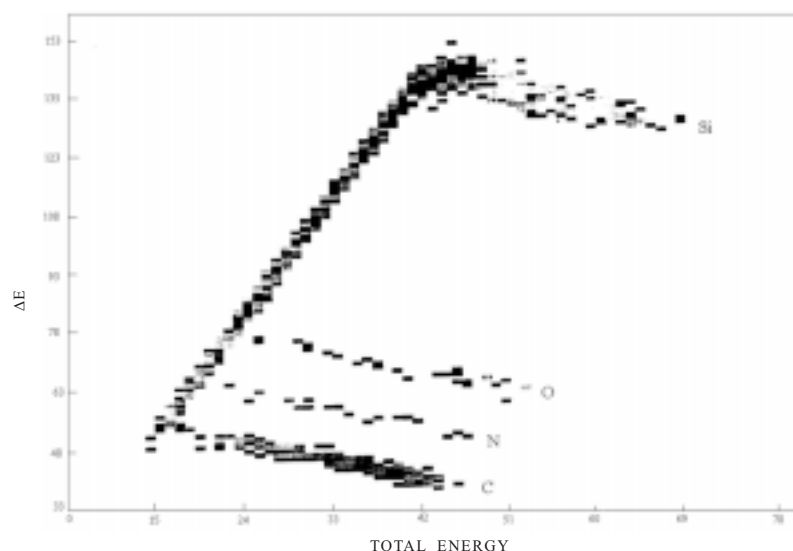


Figure 1. Typical 2-D ERDA spectra of amorphous carbon film. Y-axis represents the total recoil energy and ΔE represents a small amount of energy loss in the initial part of the detector telescope⁶.

is the difference in corresponding fluence (ions/cm²) values. The methodology for fluence-dependent areal concentration analysis and determination of sputtering yield^{5,6,14}. The structural analysis and surface morphology of the films were studied by Raman spectroscopy and atomic force microscopy (AFM).

3. RESULTS AND DISCUSSION

A typical Raman spectrum of amorphous carbon film is shown in Fig. 2. It shows two distinct peaks; one at ~1570 cm⁻¹ and another at ~1355 cm⁻¹, which are the characteristics Raman lines of amorphous carbon¹⁷. AFM image of the same film is shown in Fig. 3, which shows nanogranular nature of this film. Similar nanogranular surface of *CuO* film is observed by AFM as shown in Fig. 4. The main reason behind choosing nanostructured films in the present study was because of pronounced effect of swift heavy ion on nanophase materials. From the fluence-dependent areal concentration studies, the sputtering yields of carbon Y_C from a-C:H film and that of oxygen Y_O from *CuO* films are calculated for different S_e values and are plotted in Figures 5 and 6 respectively. The Y_C, Y_O values and corresponding

S_e, S_n values for different ion and energies are shown in Table 1.

Two important results that emerge out from this study: (i) large electronic sputtering of carbon and oxygen (as shown in the figures), increases with increase in S_e , (ii) higher yield of carbon from a-C:H film obtained as compared to oxygen from *CuO*. The loss of H from a-C:H film has already been studied⁵. The present results are understood on the basis of thermal spike model and are discussed below:

As it is evident from Table 1 that S_e is much higher (several hundred times) compared to S_n in all the cases, the resulting large sputtering is definitely mediated by electronic energy loss. Moreover, sputtering yield calculated from SRIM and the theory based on collision process^{1,16} is quite low (few atoms/ion), and hence, establishes that

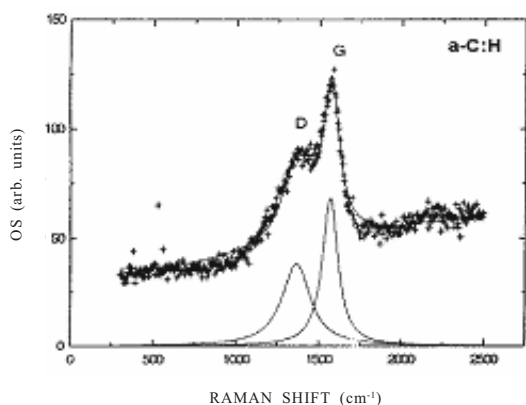


Figure 2. Typical Raman spectrum of a-C:H film indicating D and G characteristic bands.

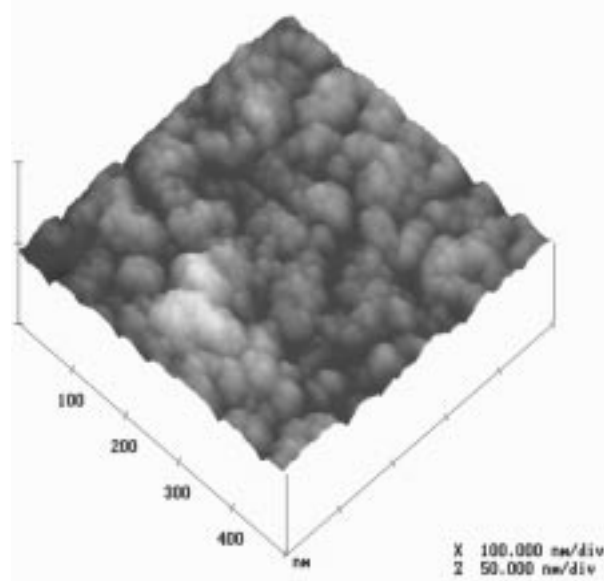


Figure 4. AFM image of *CuO* film surface.

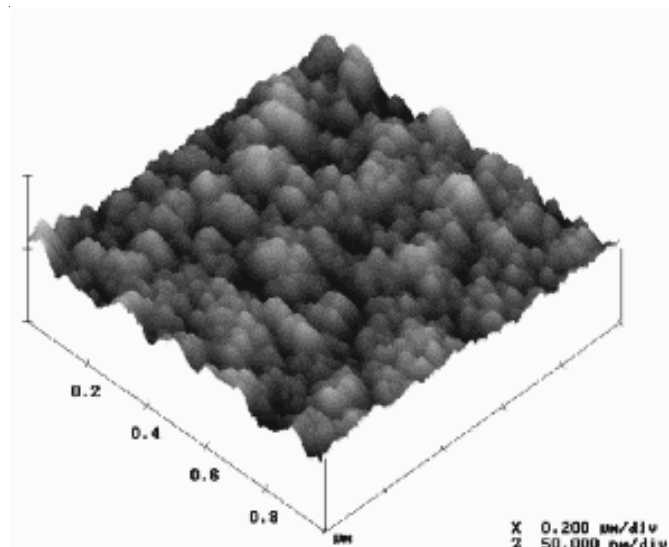


Figure 3. AFM image of a-C:H film surface.

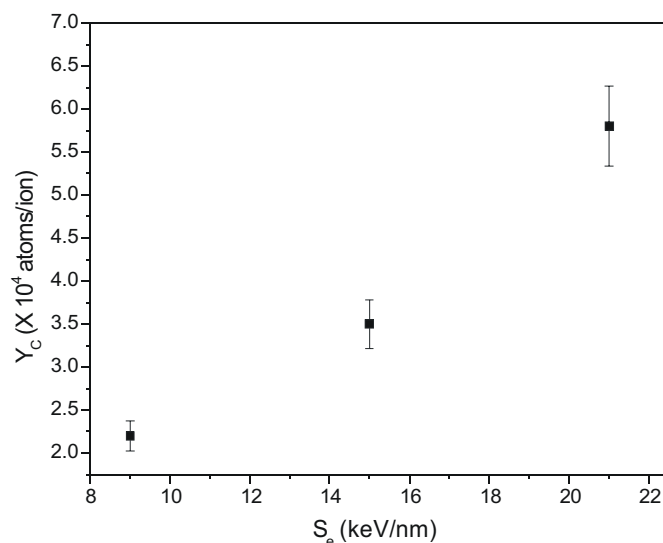


Figure 5. Sputtering yield of C (Y_C) from a-C:H films for different S_e values.

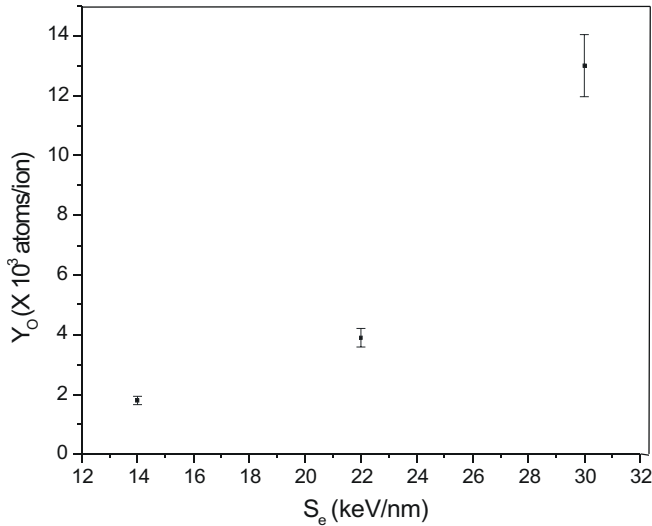


Figure 6. Sputtering yield of O (Y_o) from CuO films for different S_e values.

S_n does not play any role in large sputtering in this energy regime. Therefore, it is important to understand the energy loss process of incident ion inside the material and its subsequent effects. From thermal spike model, it can be considered that the energy deposited in the electronic subsystem gets quickly coupled to the lattice subsystems via a complex electron-phonon coupling mechanism, resulting thermalisation of the later in picosecond time scale⁷. The energy diffusion in the electronic and lattice subsystem at time t and at a distance r from the ion track, assuming cylindrical geometry is described by two coupled differential equations⁷

$$C_e \frac{\partial T_e}{\partial t} = \nabla(K_e \nabla T_e) - g(T_e - T) + B(r, t)$$

$$\rho C(T) \frac{\partial T}{\partial t} = \nabla(K(T) \nabla T) + g(T_e - T) \quad (3)$$

where, T_e , T , C_e , $C(T)$ and K_e , $K(T)$ are the temperature, the specific heat and the thermal conductivity of the electronic and atomic systems, respectively, ρ is the specific mass of the lattice and g is the electron-phonon ($e-p$) coupling constant. $B(r, t)$ is the energy density supplied by the incident ion to the electronic system at radius r and time t .

The initial energy density $B(r, t)$ can be represented by⁸

$$B(r, t) = bS_e G(t) F(r) \quad (4)$$

where bS_e is the fraction of electronic energy loss, $F(r)$ is the spatial and $G(t)$ is the temporal energy distribution function.

Electron-phonon coupling, g is a free parameter in this model and represents the strength of interaction between the excited electrons and phonons. This is inversely proportional to the electron-atom relaxation time (τ) by the relation.

$$g = \frac{\rho C_e}{\tau} \quad (5)$$

Based on thermal spike model, the electronic sputtering yield (Y) is calculated by determining temperature profile at the surface of a material, and then evaluating it using the formula¹⁰

$$Y = \int dt \int dA \Phi(T, U) \quad (6)$$

where, A is the cross sectional area from where sputtering takes place, Φ is the flux of evaporating atoms, which depends on the temperature profile T and surface binding energy U . Based on this formula, detailed derivation of sputtering yield was performed by Johnson and Evatt¹⁸ and later modified by Sigmund and Claussen¹⁰. Here we will calculate the sputtering yield based on Sigmund and Claussen model. According to this model the sputtering yield is.

$$Y = 0.041 \left(\frac{2\pi n r^2 k_B T_0}{U} \right)^2 \left[1 - \frac{3}{2} \left(\frac{U}{k_B T_0} \right)^2 \right] \quad (7)$$

where, n is the atomic density, r is the radius of ion damage zone from where material erosion takes place, k_B is the Boltzmann constant and T_0 is the spike temperature.

Here, two most important physical quantities are r and T_0 . Toulemonde,⁷ *et al.* calculated the radius of cylindrical amorphised zone inside the material created by ion, considering the appearance of a molten phase due to thermal spike and its rapid ($\sim 10^{13}$ K/s to 10^{14} K/s) quench⁷. Based on this theory, the same group has calculated the track radius to be ~ 4.8 nm, in case of $a-C:H$ for the S_e value of ~ 11.5 keV/nm. For an approximate estimation of sputtering yield, let this value be considered as r in the present case. It has been mentioned that the threshold of S_e for electronic sputtering of carbon is 250 eV/Å and the corresponding temperature⁴ is ~ 3000 K. Considering a linear relation of

Table 1. Sputtering yields, Y_c , Y_o , corresponding electronic and nuclear energy losses and incident ions with different ions and energies

Sample name	Ion and energy (MeV)	Electronic energy loss (S_e) (keV/nm)	Nuclear energy loss (S_n) (keV/nm)	Sputtering yields: Y_c and Y_o , ($\pm 10\%$) (atoms/ion)
a-C:H	Ni ⁸⁺ , 80	9.0	0.01	2.2×10^4
	Ag ¹³⁺ , 150	15.0	0.04	3.5×10^4
	Au ¹⁵⁺ , 200	21.0	0.14	5.8×10^4
CuO	Ni ⁸⁺ , 80	14.0	0.03	1.8×10^2
	Ag ¹³⁺ , 150	22.0	0.08	3.9×10^2
	Au ¹⁵⁺ , 200	30.0	0.27	1.3×10^3

lattice temperature rise with S_e as suggested by Yavinskii¹⁹, it was estimated the lattice temperature to be ~ 15681 K corresponding to the present S_e value (15 keV/nm), while the sublimation temperature of carbon is 3652 K (i.e., 0.3 eV)²⁰. Taking $n = 0.1/\text{\AA}^3$, one gets the sputtering yield of carbon from equation (7) $\sim 1.4 \times 10^6$ at./ion.

Though from this model, a large sputtering yield is realised, there is a significant mismatch with Y_C ($\sim 3.5 \times 10^4$ at./ion) value found from our experiment. This is due to the fact that the sputtering yield strongly depends on the structure of a-C:H network⁵. One also needs to consider the influence of pressure pulse generated due to large temperature spike in the lattice²¹. There could be some possibility that the temperature is carried away in the solid medium from the core, and therefore, the theoretically estimated temperature is an overestimation for the calculation of the sputtering yield. One needs to modify it considering the properties of the solid and hence demands detail investigation. Based on Eqn (6), Y_o for copper oxide can be calculated, provided the r and T_o values are known. Generally, incorporation of H in the amorphous carbon network makes the network polymeric and softer and hence in case of a-C:H film sputtering yield is larger as compared to CuO. As electronic energy loss is the main source of temperature in the lattice, the increase in sputtering yield for higher S_e values is obvious. However, to scale the sputtering yield with S_e , the exact knowledge of the following parameters, (i) atomic number density, (ii) melting temperature and (iii) heat of melting and (iv) sound velocity in the medium is important. Moreover, the effect of pressure^{21,22} over thermal spike has to be considered, which needs further experimental and theoretical studies.

5. CONCLUSIONS

Erosion of carbon from a-C:H film and depletion of oxygen from CuO at different electronic energy losses S_e is studied by online elastic recoil detection analysis. It is observed that (i) the electronic sputtering yield is appreciably high in both the cases and increases with increase in S_e , (ii) yield of C from a-C film is higher as compared to O from CuO. The results are explained on the basis of thermal spike model. Sputtering yield based on the theoretical calculation overestimates the present experimental results, and hence, a detailed investigation is required in this direction.

ACKNOWLEDGEMENTS

The author would like to thank the Physics Department of IIT Delhi, New Delhi. Accelerator Group of IUAC, New Delhi, and Gintic Institute of Technology, Singapore, for providing experimental facilities and important suggestions. Special thanks are due to Dr D. K. Avasthi, IUAC, New Delhi, for his useful suggestions.

REFERENCES

1. Sigmund, P., Theoy of sputtering. I. sputtering yield of amorphous an polycrystalline targets, *Phys. Rev.* 1969, **184**, 383-416.

2. Johnson, E. & Sundqvist, B.U.R., Electronic Sputtering: From Atomic Physics to Continuum Mechanics, *Physics Today*, 1992, March, p. 28.
3. Aumayr, F. & Winter, H.P., Potential sputtering, *Philosophical Transactions of the Royal Society London A* 2004, **362**, 77-102.
4. Pawlak, F.; Dufour, Ch. ; Laurent, A. ; Paumier, E. ; Perrière, J. ; Stoquert, J.P. & Toulemonde, M., Carbon sputtering of polymer-like amorphous carbon by swift heavy ions. *Nucl. Instr. & Meth. Phys. Res. B*, 1999, **151**, 140-45.
5. Ghosh, S.; Ingale, A.; Som, T.; Kabiraj, D.; Tripathi, A.; Mishra, S.; Zhang, S.; Hong, S. & Avasthi, D. K. Structural effects on electronic sputtering of hydrogenated amorphous carbon films. *Sol. Stat. Comm.* 2001, **120**, 445-50.
6. Ghosh, S.; Tripathi, A.; Som, T.; Srivastava, S.K.; Ganesan, V.; Gupta, A. & Avasthi, D. K. Nitrogen evolution from copper nitride films by MeV ion impact. *Radiat. Eff. and Def. in Sol.*, 2001, **154**, 151-63.
7. Toulemonde, M.; Dufour, C.; & Paumier, Transient thermal process after a high-energy heavy ion irradiation of amorphous metals and semiconductors. *E. Phys. Rev. B*, 1992, **46**, 14362-4369.
8. Mieskes, H. D.; Assmann, W.; Grüner, F.; Kucal, H.; Wang, Z. G. & Toulemonde, M., Electronic and nuclear thermal spike effects in sputtering of metals with energetic heavy ions. *Phys. Rev. B*, 2003, **67**, 155414-55425.
9. Toulemonde, M.; Assmann, W.; Trautmann, C. & Grüner, F., Jet like components of sputtering of sputtering of LiF with swift heavy ions. *Phys. Rev. Lett.*, 2002, **88**, 057602-1- 057602-4.
10. Sigmund, P. & Claussen, C., Sputtering from elastic-collision spikes. *J. Appl. Phys.*, 1981, **52**, 990-993.
11. Jakas, M., A note on thermal spikes and sputtering yields. *Radiat. Eff. and Defects in Sol.*; 2000, **152**, 157-63.
12. Ghosh, S.; Avasthi, D. K.; Som, T.; Tripathi, A.; Kabiraj, D.; Ingale, A.; Mishra, S.; Zhang, S. & Hong, X. Structure dependent electronic sputtering of a-C:H films. *Nucl. Instr. Meth. Phys. Res. B*, 2002, **190** 164-68.
13. Avasthi, D. K.; Assmann, W.; Huber, H.; Mieskes, H. D. & Nolte, H., On line monitoring of ion induced modifications by ERDA using a large area position sensitive detector telescope. *Nucl. Instr. Meth. Phys. Res. B*, 1998, **142**, 117-21.
14. Ghosh, S.; Avasthi, D. K.; Tripathi, A.; Kabiraj, D.; Sugathan, P.; Chaudhary, G. K. ; & Barua, P. Heavy ion elastic recoil detection analysis set up for electronic sputtering studies. *Rad. Eff. & Def in Sol.*, 2006, **161**, 247-55.
15. Ghosh, S.; Avasthi, D. K.; Shah, P.; Ganesan, V.; Gupta, A.; Sarangi, D.; Bhattacharya, R. & Assmann, W. Deposition of thin films of different oxides of copper by RF reactive sputtering and their

- characterization. *Vacuum*, 2000, **57**, 377-85.
16. Ziegler, J. F.; Biersack, J. P. & Littmark, U. The stopping Power of Ions in Solids, (Pergamon Press, Oxford, 1980).
 17. Schwan, J.; Ulrich, S.; Batori, S.; Ehrhardt, H. & Silva, S. R. P., Raman spectroscopy on amorphous carbon films, *J. Appl. Phys.*, 1996, **80**, 440-46.
 18. Johnson, R. E. & Evatt, Thermal spike and sputtering yields. *R. Rad. Eff.*, 1980, **52**, 187-90.
 19. Yavlinskii, Yu. N., Heating of crystalline and amorphous metals under swift heavy ion irradiation. *Rad. Eff. Def. Sol.*, 2000, **153**, 75-91.
 20. CRC Handbook of Chemistry and Physics, Ed. R.C. Weast, 67th edition (1986-1987) E-55.
 21. Jakas, M. M. & Bringa, E. M. Thermal-spike theory of sputtering: the influence of elastic waves in a one dimensional cylindrical spike. *Phys. Rev. B*, 2000, **62**, 824-30.
 22. Jakas, M. M., Fluid dynamics calculation of sputtering. *Nucl. Instr. & Meth. Phys. Res. B*, 2002, **193**, 727-33.

Contributor



Dr Santanu Ghosh is currently an Assistant Professor in the Department of Physics, Indian Institute of Technology Delhi, New Delhi. He obtained his PhD in Physics from Nuclear Science Centre, New Delhi. His present research interests are Thin Films, Nanodimensional growth of materials, Ferromagnetic semiconductor, Magnetic nanocomposites and modification of materials with energetic ions. He has more than 35 research papers published to his credit. Presently, he is with Nano-Science & Technology Group.